International Conference on Applied Energy 2019
Aug 12-15, 2019, Västerås, Sweden
Paper ID: 343

EFFECT OF BOWL-IN-PISTON CHAMBER ON THE COMBUSTION PROCESS IN A STOICHIOMETRIC NATURAL-GAS SPARK-IGNITION ENGINE

Christopher Ulishney[1], Jinlong Liu[1], Cosmin Emil Dumitrescu [1*], Ali Sivri[1]

[1] Department of Mechanical and Aerospace Engineering, West Virginia University, Morgantown, WV 26506, USA

ABSTRACT

Natural gas is a cleaner fuel source alternative for heavy duty engines. This study discusses the conversion of a single-cylinder diesel research engine to a natural-gas spark-ignited engine with port fuel injection. The conversion to spark-ignited natural-gas operation may be performed with small modifications to the engine. The piston bowl geometry of the converted engine was shown to have a substantial effect on the apparent heat-release rate, showing a double peak for certain spark timings. Peak indicated efficiency was reported at 36 percent for spark timing of -10 CA ATDC, with peak IMEP of 8 bar occurring at -15 CA ATDC. The end of combustion characteristics for the bowl-in-piston engine geometry were strongly influenced by the final flame propagation in the squish band region.

Keywords: Natural gas engine; spark ignition; stoichiometric operation; combustion characteristics; flat engine head and bowl-in-piston chamber

NONMENCLATURE

Abbreviations	
ATDC	After top dead center
CA	Crank angle
CI	Compression ignition
COV_{IMEP}	Coefficient of variation in IMEP
HRR	Heat-release rate
IMEP	Indicated mean effective pressure
MBT	Maximum brake torque
MFB	Mass fraction burned
TDC	Top dead center
SI	Spark ignition
ST	Spark timing

INTRODUCTION

Natural gas (NG) is a promising alternative fuel due to its low hydrogen to carbon ratio, which produces less carbon dioxide per kilowatt hour as compared to traditional fuels [1]. NG has a lower cost on a unit-energy basis and is readily available in most regions of the world [2]. The primary gas in the NG composition is methane, followed by ethane, propane, butane, carbon monoxide, carbon dioxide, and nitrogen. After purification, common pipeline end-use NG consists of between 87-96 percent methane [3].

NG is an inherently knock resistant fuel, which requires high compression ratios or spark assistance to ignite. However, even under the high compression ratios characteristic of diesel engines it is not easy to control NG autoignition. As a result, the conversion of a diesel engine to NG spark ignition (SI) operation requires the use of a spark plug or a secondary, more reactive fuel, to act as an ignition source for the gas [4]. The first conversion solution is more economic [5] and the object of this study. There are few existing studies that detail stoichiometric combustion operation in compression ignition (CI) engines converted to NG SI operation, as most of them focused on NG SI engines derived from gasoline engines [6]. The goal of this research is to further the understanding of the combustion process in the CI-to-SI converted engines, which can accelerate the adoption of similar technologies. For example, a literature reviewed showed that the traditional SI engine geometry (i.e., pent-roof chamber) produces a different flow motion and turbulence intensity compared to a diesel chamber [7]. But there are not many other studies in the literature that presented and/or discussed NG premixed combustion inside a bowl-in-piston chamber. Therefore, this work is one of the first to report some of

Selection and peer-review under responsibility of the scientific committee of the 11th Int. Conf. on Applied Energy (ICAE2019).

the unique effects of the piston bowl geometry on the combustion process of a diesel engine converted to NG SI operation.

EXPERIMENTAL SETUP

The single-cylinder research engine (Riccardo, Model Proteus) was converted to operate with natural-gas under spark-ignition conditions, then tested using 99 vol.% methane. A 2-inch laminar flow element (Meriam, Model Z50MC2-2) and pressure transducer (Heise, Model PTE-1) were used to determine the intake air flow. The fuel flow was controlled with a mass flow controller (Alicat, Model MCRW-500SLPM). The time averaged equivalence ratio was determined using West Virginia University (WVU)'s proprietary data logging software (Scimitar), which was capable of time averaging the unsteady fuel flow with a five second lagging average. Engine coolant and oil temperatures were monitored using k-type thermocouples (Omega) connected to a data logger (ICPDAS, Model PET-7019Z) and kept constant throughout experiments. In-cylinder pressure was measured using a piezo-electric pressure transducer (Kistler, Model 6125C). The air pressure inside the intake manifold was measured and used to peg in-cylinder pressure. A DC dynamometer was used for motoring and loading the engine. The spark plug was mounted in the diesel injector position and controlled using an external engine control unit (Megasquirt, Model 3X) with its controlling software (Tunerstudio MS, Version 3.0.28) A schematic of the experimental setup is shown in Figure 1. Table 1 shows engine specifications and operating conditions. More detailed information about the engine setup can be found in reference [1].

Table 1. Engine specifications and operating conditions

Bore x Stroke	130.2 x 150 [mm]
Connecting rod length	275 [mm]
Compression ratio	13.3
Speed	900 RPM
Equivalence ratio	1 (stoichiometric)
Spark timing (ST)	-35 to -5 CA ATDC

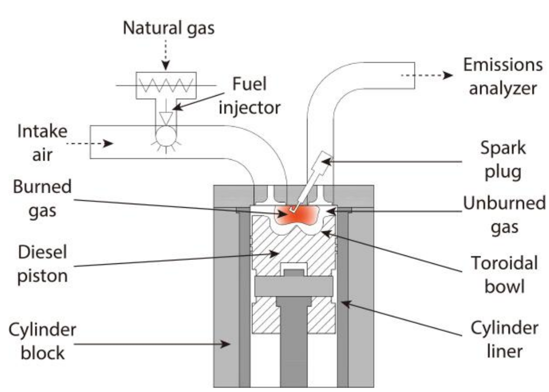

Figure 1. Engine schematic

RESULTS AND DISCUSSION

A minimum of 100 cycles were collected for analysis of each operating condition, filtered and averaged using MATLAB®.

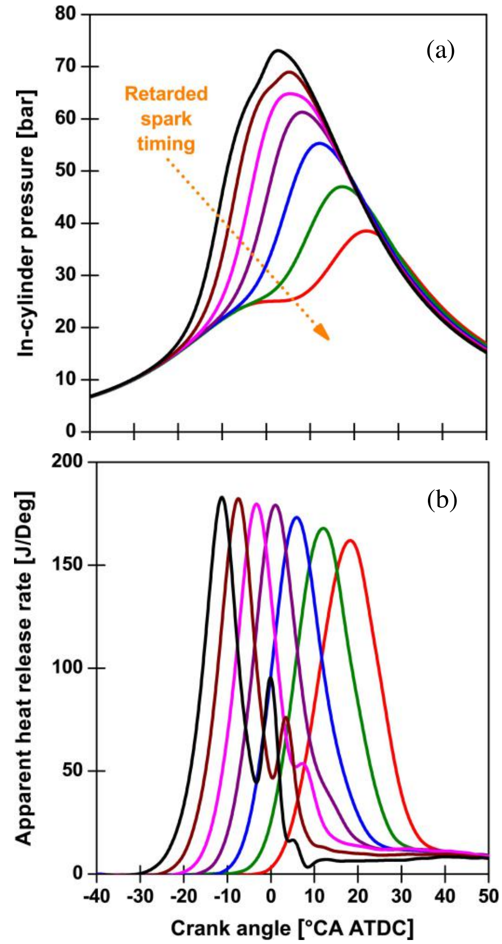

Figure 2. Effect of spark timing on (a) in-cylinder pressure and (b) apparent heat-release rate

Indicated data in Figure 2a shows the effects of spark timing on in-cylinder pressure under stoichiometric conditions at 900 RPM, using methane as fuel. For methane operation in a lower compression-ratio diesel engine, the transition to spark ignition was required. The engine was tested under stoichiometric conditions to be representative of engine performance under high load. Advancing ST increased the peak pressure-rise rate to ~ 4.5 bar/deg. The maximum in-cylinder pressure occurred with the most advanced ST of -35 CA ATDC, slightly after TDC. The peak pressure incrementally shifted away from TDC later into the expansion stroke, as the spark timing was retarded. Figure 2b shows the apparent heat-release rate (HRR) at each ST condition, with a similar incremental shift in the location of the HRR peak to the ST change.

The second HRR peak seen at the most advanced ST was due to an important fuel fraction that trapped inside the squish and burned after the rapid-burning process [8]. Moreover, advancing ST increased the mass fraction inside the squish and therefore affected the engine thermal efficiency due to the less optimal burning conditions there (lower temperature), which contributed to a higher magnitude of the second HRR peak [1, 8]. The -35 CA ATDC ST case had a triple HRR peak because the burning stage inside the squish was divided into two stages, separated by the compression and expansion strokes. The large fuel fraction inside the squish burned slowly, which increased the potential to knock. Experiments indicated there was no knocking from -30 to -5 CA ATDC ST. However, under the -35 CA ADTC ST condition occasional knocking cycles appeared.

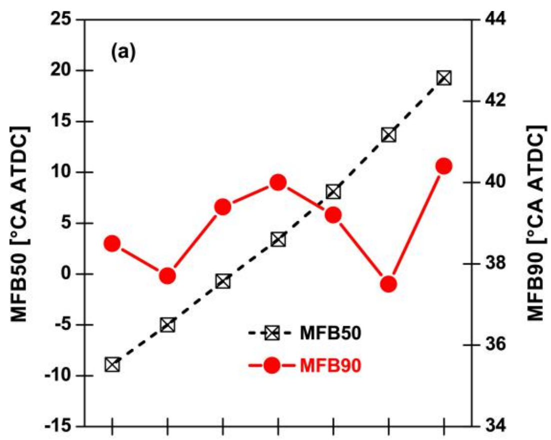

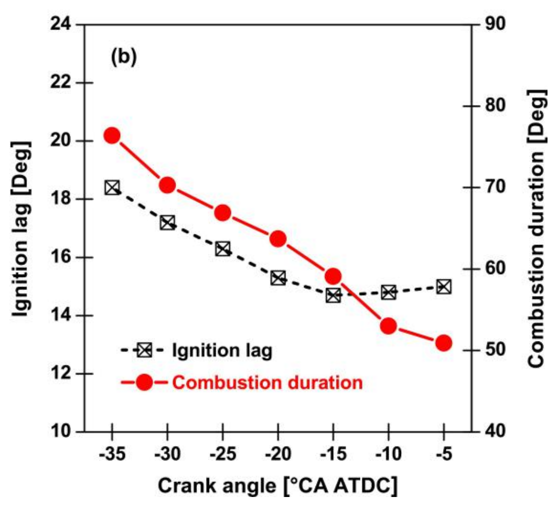

Figure 3. Effect of spark timing on (a) MB50 and MB90 and (b) ignition lag and combustion duration

MFB90 was not heavily affected by the ST, as illustrated in Figure 3a. Such phenomena occurred probably due to the squish-burn process which was also almost completed at MFB90 [1]. In other words, the late combustion was due to the important fuel-air mixture mass trapped inside the crevice region. MFB50 keeps the same phasing as the ignition setting, however MFB90 changes due to the influence of longer squish burn duration. Excess burning in the squish should be avoided due to the higher heat transfer rates to cylinder walls, which in turn lowers engine efficiency.

Ignition lag was defined here as the difference between ST and MFB10 [7]. The trend shown in Figure 3b indicates a minimum ignition lag of 15 CAD for the -15 CA ATDC ST. Combustion duration, also shown in Figure 3b, was defined as the difference between MFB5 and MFB95 [7]. The combustion duration steadily decreased as spark timing was retarded. Longer combustion durations are associated with increased heat loss as well as higher production of thermal nitrogen oxides. MFB95 was too delayed for comparison. The ignition lag for ST -15 CA ATDC shows ignition occurring at TDC, resulting in the highest IMEP.

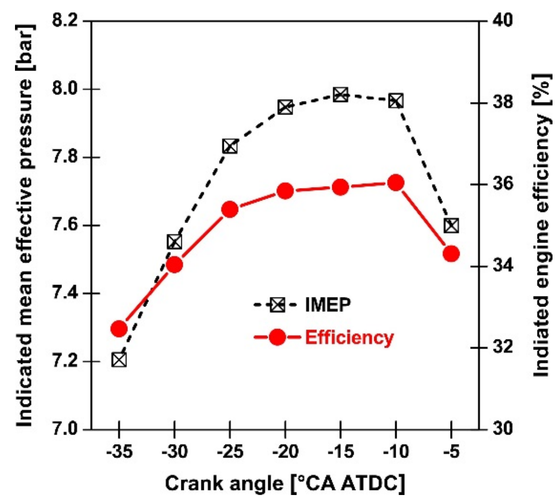

Figure 4. Effect of spark timing on indicated mean effective pressure and thermal efficiency

The peak locations of IMEP and thermal efficiency shown in Figure 4 suggest that maximum brake torque (MBT) timing was between -15 and -10 CA ATDC. Peak indicated thermal efficiency was 36% for -10 CA ATDC ST, while peak IMEP of 8 bar was for -15 CA ATDC ST. The peak operation points also showed the lowest ignition delay, caused by higher temperature and pressure during the development of the ignition kernel.

While the MBT timing had the two-stage combustion process, there was no dual-peak HRR seen in the mean cycle. However, individual cycles showed an HRR “bump” after the main HRR peak. Moreover, as there was no knocking observed at the MBT condition, this 13.3 compression ratio engine can operate at stoichiometric operation, at least for the conditions investigated here. The addition of more easily igniting sub-components of NG may reduce the knock-resistance at such operating conditions.

Both advanced and retarded ST operations had higher cycle-to-cycle variations. However, the COV_{IMEP} for all conditions were below 1.5%, despite the slow laminar flame speed of NG. Such stable combustion can be attributed to the "fast-burn" chamber.

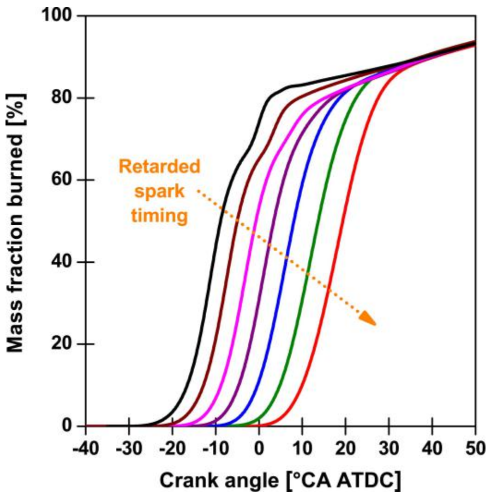

Figure 5. Effect of spark timing on mass fraction burned

Figure 5 indicated a slow burn process followed by the rapid burning event, which was more evident in advanced ST operation. The combustion phasing is shown to remain evenly spaced until MFB60, at which point deviation occurs until all approach the same end of combustion mode near MFB85. The change in combustion phasing indicates that the slow burning in the squish band increased the overall combustion process for advanced ST, which would likely have negative impacts on the formation of nitrogen oxides.

SUMMARY AND CONCLUSIONS

This study provides useful insight into the combustion process of a single-cylinder research CI engine (13.3 compression ratio) converted to port injection NG SI operation. Experiments that investigated combustion characteristics at stoichiometric conditions, 900 rpm, and various spark timings were performed using methane as fuel. The main conclusions were:

- CI engines can be converted to NG SI operation with relatively small modifications.
- Bowl-in-piston geometry played a critical role in the flame development and propagation inside the CI engines converted to NG SI operation.
- Peak indicated efficiency of 36% occurred for -10 CA ATDC ST, while peak IMEP of 8 bar occurred at -15 CA ATDC ST.
- The change in combustion phasing mimics the change in spark timing until MFB50, at which point combustion in the squish region controlled the end of combustion.

ACKNOWLEDGEMENT

The material is based upon work funded by the WV Higher Education Policy Commission under grant number HEPC.dsr.18.7. The authors gratefully acknowledge WVU's Center for Alternative Fuels Engines and Emissions (CAFEE), WVU's Center for Innovation in Gas Research and Utilization (CIGRU), and the MAE department for their support and assistance.

AUTHOR INFORMATION

*Corresponding author: West Virginia University, P.O. Box 6106, Morgantown, WV 26506, USA; tel.: 304-293-3330; fax: 304-293-6689; e-mail: cedumitrescu@mail.wvu.edu

REFERENCES

[1] Liu J, Investigation of combustion characteristics of a heavy-duty diesel engine retrofitted to natural gas spark ignition operation. Ph.D. dissertation, West Virginia University, Morgantown, West Virginia, 2018.
[2] Gupta M, Bell SR, Tillman ST. An investigation of lean combustion in a natural gas-fueled spark-ignited engine. Journal of Energy Resources Technology 1996; 118: 145-151.
[3] NAESB. Natural gas specs sheet. Available at www.naesb.org/pdf2/wgq_bps100605w2.pdf.
[4] Donateo T, Tornese F, Laforgia D. Computer-aided conversion of an engine from diesel to methane. Applied Energy 2013; 108: 8-23.
[5] Reyes M, Tinaut FV, Giménez B, Pérez A. Characterization of cycle-to-cycle variations in a natural gas spark ignition engine. Fuel 2015; 140: 752-61.
[6] Weaver CS. Natural gas vehicles - a review of the state of the art. SAE Transactions 1989; 98: 1190-210.
[7] Heywood JB, Internal combustion engine fundamentals. McGraw-Hill, New York, 1988.
[8] Liu J, Dumitrescu CE, Combustion partitioning inside a natural gas spark ignition engine with a bowl-in-piston geometry. Energy Conversion and Management 2009; 183: 73-83.

